THE IMMERSED FINITE VOLUME ELEMENT METHOD FOR SOME INTERFACE PROBLEMS WITH NONHOMOGENEOUS JUMP CONDITIONS

LING ZHU[1,2], ZHIYUE ZHANG[1], AND ZHILIN LI[3,1]

Abstract. In this paper, an immersed finite volume element (IFVE) method is developed for solving some interface problems with nonhomogeneous jump conditions. Using the source removal technique of nonhomogeneous jump conditions, the new IFVE method is the finite volume element method applied to the equivalent interface problems with homogeneous jump conditions and have properties of the usual finite volume element method. The resulting IFVE scheme is simple and second order accurate with a uniform rectangular partition and the dual meshes. Error analyses show that the new IFVE method with usual $O(h^2)$ convergence in the L^2 norm and $O(h)$ in the H^1 norm. Numerical examples are also presented to demonstrate the efficiency of the new method.

Key words. Elliptic interface problem, non-homogeneous jump conditions, immersed finite volume element.

1. Introduction

Interface problems are often encountered in many important physical and industrial applications [11, 17].

In this paper, we consider the Poisson equation in a bounded Ω with an interface Γ in the domain,

$$(1) \qquad -\Delta u = f \quad (x,y) \in \Omega \backslash \Gamma \subset R^2,$$

with a Dirichlet boundary condition

$$(2) \qquad u(x,y) = g(x,y) \quad (x,y) \in \partial\Omega,$$

and jump conditions

$$(3) \qquad [u]_\Gamma = w,$$

$$(4) \qquad [u_n]_\Gamma = Q,$$

where

$$[u]_\Gamma = \lim_{\substack{(x,y)\to\Gamma \\ (x,y)\in\Omega^+}} u(x,y) - \lim_{\substack{(x,y)\to\Gamma \\ (x,y)\in\Omega^-}} u(x,y), \quad [u_n]_\Gamma = \lim_{\substack{(x,y)\to\Gamma \\ (x,y)\in\Omega^+}} u_n - \lim_{\substack{(x,y)\to\Gamma \\ (x,y)\in\Omega^-}} u_n,$$

with the notation $u_n = \nabla u \cdot n$. The interface $\Gamma \in C^2$ is a curve separating Ω into two subsets Ω^+ and Ω^-, and n is the unit outward normal vector of Γ pointing to the Ω^+ side, see Fig. 1 for an illustration.

In this paper, we assume that $w \neq 0$ and $Q \neq 0$. That is why we call such a problem that has nonhomogeneous jump conditions. The jump conditions can be obtained from the physics or mathematical derivations. For example, in Peskin's
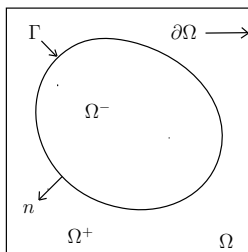
FIGURE 1. A diagram of the domain for the interface problem.

immersed boundary (IB) model [22], the pressure and its gradient are discontinuous, while the velocity is continuous, but the normal derivative of the velocity is discontinuous.

There are variety of methods that can be applied to solve the interface problem (1)-(4) numerically. First of all, in terms of the meshes, one can use a body fitted mesh or an unfitted mesh. With a body fitted mesh, the standard finite element method or finite volume element method is straightforward when $w = 0$. In this paper, we discuss a new finite volume element method using a uniform mesh with which there is almost no cost in the mesh generation; and we can utilize a fast Poisson solver, for example, the one from Fishpack [1]. Thus here we only give a brief literature review on numerical methods using a uniform unfitted mesh.

When $w = 0$, then the problem can be written as

$$-\Delta u(\mathbf{x}) = f(\mathbf{x}) - \int_\Gamma Q(\mathbf{X}(s))\delta(\mathbf{x} - \mathbf{X}(s))ds, \quad \mathbf{x} \in \Omega,$$

$$u(\mathbf{x}) = g(\mathbf{x}), \ \mathbf{x} \in \partial\Omega,$$

where $\mathbf{X}(s) \in \Gamma$. In this case, we can use Peskin's IB method [22] to solve the interface problem. IB method is first order accurate and usually requires that the solution is continuous to have a convergent result. The immersed interface (II) method [12] is a second order accurate finite difference method even if $w \neq 0$ and $Q \neq 0$. To solve the resulting linear finite difference equations, both IB method and II method can call a fast Poisson solver. The main difference between the two methods are the right hand sides and the convergence rates. Related other methods include the matched interface and boundary (MIB) method [25], the ghost fluid (GF) method [3,19], the virtual node algorithm [2]. Another type of methods is based on finite element formulation. One type of approaches is to add some enrichment function near the interface [23] in which the number of degree of the freedom will be changed. Our method is more related to the immersed finite element (IFE) method [7, 14, 16] for which the structure and the number of degree of the freedom remain unchanged. IFE method has been applied to interface problems with nonhomogeneous jump conditions in [7, 9, 10, 24]. In [7, 15, 18], the source removal technique was developed for treating nonhomogeneous jump conditions. In [10], a weak formulation inspired by the boundary condition capturing method [20] is proposed. In [24], the locally modified triangulations on irregular domains are proposed.

In this paper, we develop the *immersed finite volume element* (IFVE) method which is based on IFE method, similarly to [5,8]. The finite volume element method is also called generalized difference method [13]. Because the finite volume element

method can preserve the mass conservation law and many important physical quantities. Compared with previous work of IFVE method [5, 8], the new developed IFVE method in this paper can deal with non-homogeneous jump conditions.

The basic idea in IFVE method for the interface problem is that the standard finite volume element method is used away from the interface and the finite volume element schemes are modified locally near or on the interface according to the interface relations. In [5, 8], the basis functions in the finite element space are reconstructed to satisfy the jump conditions on the interface as accurately as possible. Here, we introduce a formulation which is based on the extension of the jump conditions (3) and (4) along the normal lines like IFE method in [7, 15, 18]. By the formulation, we transform the interface problem to a problem with a smooth solution and only need to use the usual finite element basis functions. Unlike IFE method in [7] which only need to treat the non-interface elements and interface elements, one of the difficulties of IFVE method in this paper is that we need to modify the so-called sub-interface dual elements.

The rest of this article is organized as follows. In section 2, we explain the source removal idea to treat nonhomogeneous jump conditions. In section 3, we present IFVE method that is based on the bilinear finite element. In section 4, we provide error estimates about the numerical solution. In section 5, we give two numerical examples to demonstrate features of the proposed method. In section 6, we draw some conclusions about IFVE method.

2. The source removal technique of nonhomogeneous jump conditions

Our idea of the new method is to apply the source removal technique for nonhomogeneous jump conditions developed in [7,15,18] before applying the finite volume element method. In this section, we briefly explain the source removal technique. We assume that $w \in C^2(\Gamma)$ and $Q \in C^2(\Gamma)$. Let the interface Γ be represented by the zero level set of a Lipschitz continuous function $\varphi(x, y)$, that is,

$$(5) \qquad \varphi(x, y) \begin{cases} < 0 & \text{if } (x, y) \in \Omega^-, \\ = 0 & \text{if } (x, y) \in \Gamma, \\ > 0 & \text{if } (x, y) \in \Omega^+. \end{cases}$$

We assume that $\varphi(x, y) \in C^2(\Omega)$ and $|\nabla \varphi(x, y)| \neq 0$ in a neighborhood of the interface Γ. The signed distance function is such a function. In a neighborhood of the interface Γ, we define the extensions of $w(x, y)$ and $Q(x, y)$ along the normal line (in both directions) by

$$w_\rho(x, y) = w_\rho((X, Y) + \alpha(p_1, p_2)) = w(X, Y) \quad (X, Y) \in \Gamma,$$

$$Q_\rho(x, y) = Q_\rho((X, Y) + \alpha(p_1, p_2)) = Q(X, Y) \quad (X, Y) \in \Gamma,$$

where $p = (p_1, p_2) = (\varphi_x, \varphi_y)$ (note that $n = p/|p|$), and the scalar α is determined from the following quadratic equation,

$$\varphi(x, y) + (\nabla \varphi(x, y) \cdot p)\alpha + \frac{1}{2}(p^T He(\varphi(x, y))p)\alpha^2 = 0,$$

where

$$p^T He(\varphi(x, y))p = \varphi_x^2 \varphi_{xx} + 2\varphi_x \varphi_y \varphi_{xy} + \varphi_y^2 \varphi_{yy}.$$

The values of $\varphi(x, y)$, φ_x, φ_y, $\cdots$, φ_{yy} are approximated using the standard second order finite difference at the grid point (x, y). Usually there are two solutions of α, we choose the one such $(X, Y) + \alpha(p_1, p_2)$ is closer to the interface.

We construct $u_\rho : \Omega \to R$ based on the extensions,

$$(6) \qquad u_\rho(x,y) = w_\rho(x,y) + Q_\rho(x,y)\frac{\varphi(x,y)}{|\nabla\varphi(x,y)|}.$$

Then we define

$$(7) \qquad \hat{u}(x,y) = H(\varphi(x,y))u_\rho(x,y) = \begin{cases} 0 & \text{if } \varphi(x,y) < 0, \\ u_\rho(x,y) & \text{if } \varphi(x,y) \ge 0, \end{cases}$$

where $H(\cdot)$ is the Heaviside function. Note that $u_\rho(x,y) \in C^2$ in the neighborhood of the interface Γ, $\hat{u}(x,y)$ has the same nonhomogeneous jumps conditions across the interface as $u(x,y)$. We refer to [7, 15, 18] for details.

The source removal technique is based on the following theorem.

Theorem 2.1. *Let $u(x,y)$ be the solution of (1) to (4) and let $\hat{u}(x,y)$ be defined in (7). If we define $q(x,y) = u(x,y) - \hat{u}(x,y) = u(x,y) - H(\varphi(x,y)u_\rho(x,y))$, then the following are true:*

$$(8) \qquad -\Delta q = f(x,y) + H(\varphi(x,y))\Delta u_\rho(x,y) \quad (x,y) \in \Omega\backslash\Gamma,$$

$$(9) \qquad [q]_\Gamma = 0, \ [q_n]_\Gamma = 0.$$

The proof can be found in [7, 15, 18].

Remark 2.1. *While $q(x,y)$ is smooth $(C^1(\Omega))$ across the interface Γ, the right-hand side of (8) is discontinuous across the interface.*

3. The immersed finite volume element method

For a rectangular domain $\Omega = (-1,1) \times (-1,1)$, we now consider a rectangular decomposition T_h consisting of closed rectangle elements K such that $\overline{\Omega} = \cup_{K \in T_h} K$. We will use N_h to denote the set of all nodes or vertices of T_h,

$$N_h = \{p : \ p \text{ is a vertex of element } K \in T_h \text{ and } p \in \overline{\Omega}\},$$

and we let $N_h^0 = N_h \cap \Omega$, which denotes the set of interior vertices.

We then introduce a dual mesh T_h^* related to T_h. The elements of T_h^* are called control volumes. In each element $K \in T_h$ consisting of vertices $\mathbf{x}_k$, $\mathbf{x}_l$, $\mathbf{x}_m$, $\mathbf{x}_n$, we take Q as the joint of the two lines connecting the midpoints of the opposite sides of the rectangle element K. This is called the central dual decomposition. Then connect Q to the midpoints by straight lines $\gamma_{kl,K}$. For a vertex $\mathbf{x}_k$ we let V_k be the rectangle whose edges are $\gamma_{kl,K}$ in which $\mathbf{x}_k$ is a vertex of the element K. We call V_k a control volume centered at $\mathbf{x}_k$. Obviously, we have

$$\cup_{\mathbf{x}_k \in N_h} V_k = \overline{\Omega}.$$

For simplicity, let the decomposition T_h is equal in the x-direction or the y-direction. See Fig. 2 for the illustration of V_k. V_k also denotes the dual element of the node $\mathbf{x}_k$.

We call the grid T_h^* regular or quasi-uniform if there exists a positive constant $C > 0$ such that:

$$C^{-1}h^2 \le \text{meas}(V_k) \le Ch^2, \text{ for all } V_k \in T_h^*.$$

Here, h is the maximal diameter of all elements $K \in T_h$.

For an arbitrary interface Γ, some of the dual elements will be cut through by Γ. There are three cases of a dual element V_k centered at a node point $\mathbf{x}_k = (x_i, y_j)$,
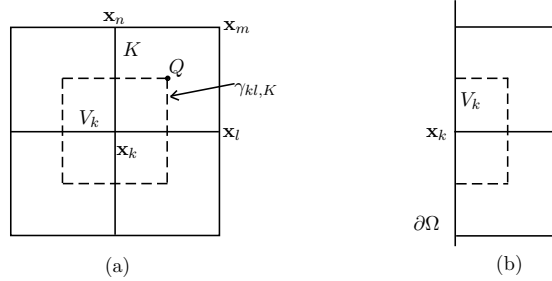
FIGURE 2. The dual element V_k centered at $\mathbf{x}_k$.

see Fig. 3 for an illustration. Type I is an non-interface dual element; Type III is an interface dual element; Type II is a sub-interface dual element, that is, the dual element V_k is not cut through by Γ, but the elements related to V_k are cut through by Γ. Here, we assume that the interface Γ intersects the edges of the elements at D and E, and approximate the arc DE by the line segment $\overline{DE}$. The area of the region enclosed by the $\overline{DE}$ and the arc DE is of order $O(h^3)$.
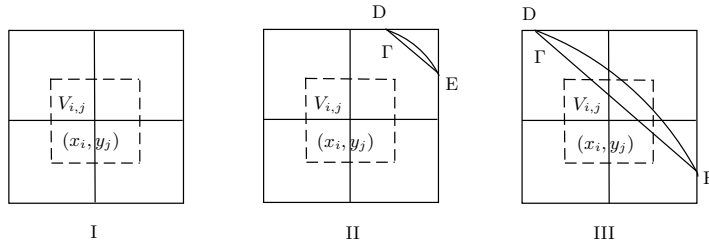
FIGURE 3. The three kinds of the dual element.

If $w = 0$ and $Q = 0$ on Γ, we integrate (1) on $V_{i,j}$, and employ the Green's formula to obtain the weak form. We need to find $u \in H^1(\Omega)$ with $u = g$ on $\partial\Omega$ such that

$$(10) \qquad -\int_{\partial V_{i,j}} \left(\frac{\partial u}{\partial x} dy - \frac{\partial u}{\partial y} dx \right) = \int_{V_{i,j}} f dx dy.$$

In this case, the standard finite volume element method can be applied.

In this paper, we focus on the case when $w \neq 0$ and $Q \neq 0$. We employ to the source removal technique [7, 15, 18] and combine the technique with the finite volume element method.

We integrate (8) on $V_{i,j}$, and employ the Green's formula to obtain

$$(11) \quad -\int_{\partial V_{i,j}} \left(\frac{\partial q}{\partial x} dy - \frac{\partial q}{\partial y} dx \right) = \int_{V_{i,j}} f dx dy + \int_{V_{i,j}} H(\varphi(x,y))\Delta u_\rho dx dy.$$

Then we introduce the bilinear finite element space $W_h \subset H^1(\Omega)$ with respect to the decomposition T_h. Let $\{\phi_{i,j}(x,y)\}$ be the bilinear nodal basis functions of the usual finite-element space W_h,

$$(12) \qquad \phi_{i,j}(x,y) = \begin{cases} \left(1 - \dfrac{|x - x_i|}{h}\right)\left(1 - \dfrac{|y - y_j|}{h}\right) & (x,y) \in R_{i,j}, \\ 0 & \text{otherwise,} \end{cases}$$

where $R_{i,j}$ is a rectangular element centered at the point (x_i, y_j).

Theorem 3.1. *There exists a unique $q_h \in W_h$ such that*

$$(13) \quad -\int_{\partial V_{i,j}} \left(\frac{\partial q_h}{\partial x} dy - \frac{\partial q_h}{\partial y} dx \right) = \int_{V_{i,j}} f dx dy + \int_{V_{i,j}} H(\varphi(x, y)) \Delta u_\rho dx dy,$$

where

$$q_h|_{V_{i,j}} = \sum_{m,n=\{-1,0,1\}} \phi_{i+m,j+n} q_{h,i+m,j+n}.$$

We rewrite (13) in terms of $u_h = q_h + \hat{u}$ to obtain the IFVE scheme:

$$(14) \quad -\int_{\partial V_{i,j}} \left(\frac{\partial u_h}{\partial x} dy - \frac{\partial u_h}{\partial y} dx \right) =$$

$$\int_{V_{i,j}} f dx dy - \int_{\partial V_{i,j}} \left(\frac{\partial \hat{u}}{\partial x} dy - \frac{\partial \hat{u}}{\partial y} dx \right) + \int_{V_{i,j}} H(\varphi(x, y)) \Delta u_\rho dx dy.$$

As shown in Fig. 3, the dual element $V_{i,j}$ of type I or type II is entirely in Ω^-, and thus the last two terms of integration over the element $V_{i,j}$ are zero since $H(\varphi(x, y)) = 0$ and $\hat{u} = 0$. If this element is entirely in Ω^+, we have

$$\int_{\partial V_{i,j}} \left(\frac{\partial \hat{u}}{\partial x} dy - \frac{\partial \hat{u}}{\partial y} dx \right) - \int_{V_{i,j}} H(\varphi(x, y)) \Delta u_\rho dx dy$$

$$= \int_{\partial V_{i,j}} \left(\frac{\partial u_\rho}{\partial x} dy - \frac{\partial u_\rho}{\partial y} dx \right) - \int_{V_{i,j}} \Delta u_\rho dx dy = 0.$$

When the dual element is Type III, the last two terms of integration are not zero in general. We define

$$u_h|_{V_{i,j}}(x, y) = \begin{cases} \displaystyle\sum_{m,n=\{-1,0,1\}} \phi_{i+m,j+n} u_{h,i+m,j+n} & \text{if } V_{i,j} \text{ is type } I \text{ or } II, \\ \displaystyle\sum_{m,n=\{-1,0,1\}} \phi_{i+m,j+n} u_{h,i+m,j+n} + \\ \displaystyle\sum_{m,n=\{-1,0,1\}} \phi_{i+m,j+n} \hat{u}(x_{i+m}, y_{j+n}) & \text{otherwise.} \end{cases}$$

As a result, if $V_{i,j}$ is type I or II, we use the following scheme

$$(15) \quad -\int_{\partial V_{i,j}} \left(\frac{\partial u_h}{\partial x} dy - \frac{\partial u_h}{\partial y} dx \right) = \int_{V_{i,j}} f dx dy.$$

If $V_{i,j}$ is type III, we use the scheme (14).

However, if we treat Type II as above, we will get wrong results since the element K_3 is cut through by the interface Γ, see Fig. 4 for an illustration. That is, on K_3, $u_h \neq \phi_{i,j} u_{h,i,j} + \phi_{i+1,j} u_{h,i+1,j} + \phi_{i+1,j+1} u_{h,i+1,j+1} + \phi_{i,j+1} u_{h,i,j+1}$. For this case, we could reconstruct the bilinear nodal basis function $\phi_{i,j}$ as described in [8]. In [8], $\phi_{i,j}$ (also $\phi_{i+1,j}$, $\phi_{i+1,j+1}$, $\phi_{i,j+1}$) is a piecewise functions with two bilinear polynomials on K_3 patched up together by the interface jump conditions. The schemes proposed in [8] is complicated and difficult to implement. Clearly, such basis functions depend on the interface location and the jump conditions. In our proposed approach, we modify the scheme without changing the basis functions.
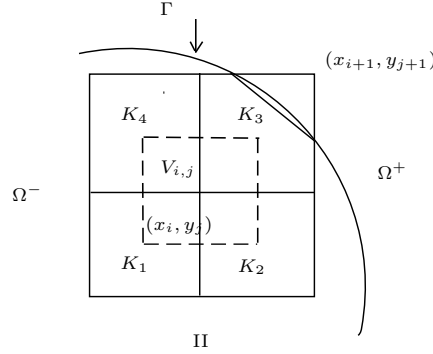
FIGURE 4. The dual element $V_{i,j}$ of Type II.

We reconsider the schemes from (13) for sub-interface dual elements. If $V_{i,j} \in \Omega^-$, then $H(\varphi(x,y)) = 0$. Hence, we have

$$(16) \qquad -\int_{\partial V_{i,j}} \left(\frac{\partial q_h}{\partial x} dy - \frac{\partial q_h}{\partial y} dx \right) = \int_{V_{i,j}} f dx dy.$$

Furthermore, we use $u_h = q_h + \hat{u}$ to get the scheme,

$$(17) \qquad -\int_{\partial V_{i,j}} \left(\frac{\partial u_h}{\partial x} dy - \frac{\partial u_h}{\partial y} dx \right) = \int_{V_{i,j}} f dx dy$$
$$+ \sum_{m,n=\{-1,0,1\}} H(\varphi(x_{i+m}, y_{j+n})) A_{i+m,j+n} u_\rho(x_{i+m}, y_{j+n}),$$

where

$$(18) \qquad A_{i,j} = -\int_{\partial V_{i,j}} \left(\frac{\partial \phi_{i,j}}{\partial x} dy - \frac{\partial \phi_{i,j}}{\partial y} dx \right).$$

Similarly, if $V_{i,j} \in \Omega^+$, then $H(\varphi(x,y)) = 1$ and we have

$$(19) \quad -\int_{\partial V_{i,j}} \left(\frac{\partial u_h}{\partial x} dy - \frac{\partial u_h}{\partial y} dx \right) = \int_{V_{i,j}} f(x,y) dx dy + \int_{V_{i,j}} \Delta u_\rho dx dy$$
$$+ \sum_{m,n=\{-1,0,1\}} H(\varphi(x_{i+m}, y_{j+n})) A_{i+m,j+n} u_\rho(x_{i+m}, y_{j+n}).$$

If we consider the local conservation property on a control volume of the finite volume element method, we can get a simpler scheme than (19). Now, we let $\tilde{q} = u + \tilde{u}$, and define

$$(20) \quad \tilde{u}(x,y) = (1 - H(\varphi(x,y))) u_\rho(x,y) = \begin{cases} 0 & \text{if } \varphi(x,y) > 0, \\ u_\rho(x,y) & \text{if } \varphi(x,y) \le 0. \end{cases}$$

(1) is written similarly as Theorem 2.1,

$$(21) \qquad -\Delta \tilde{q} = f(x,y) - (1 - H(\varphi(x,y))) \Delta u_\rho(x,y) \quad (x,y) \in \Omega \backslash \Gamma.$$

Along the interface Γ, $\tilde{q}$ also satisfies the homogeneous jump condition as follows,

$$[\tilde{q}]_\Gamma = 0, \ [\tilde{q}_n]_\Gamma = 0.$$

We integrate (21) on $V_{i,j}$ and get the numerical scheme,

$$-\int_{\partial V_{i,j}} \left(\frac{\partial \tilde{q}_h}{\partial x} dy - \frac{\partial \tilde{q}_h}{\partial y} dx \right) = \int_{V_{i,j}} f(x,y) dx dy - \int_{V_{i,j}} (1 - H(\varphi(x,y))) \Delta u_\rho dx dy,$$

where $V_{i,j}$ is a sub-interface dual element and belongs to Ω^+. Then, $(1 - H(\varphi(x, y)))$ = 0. Thus, by $\tilde{q}_h = u_h + \tilde{u}$, we have

$$(22) \quad -\int_{\partial V_{i,j}} \left(\frac{\partial u_h}{\partial x} dy - \frac{\partial u_h}{\partial y} dx \right) = \int_{V_{i,j}} f dx dy$$
$$- \sum_{m,n=\{-1,0,1\}} (1 - H(\varphi(x_{i+m}, y_{j+n}))) A_{i+m,j+n} u_\rho(x_{i+m}, y_{j+n}).$$

In (22), we avoid the computation of the term $\int_{V_{i,j}} \Delta u_\rho dx dy$ in (19). Hence, IFVE method that we proposed can be summarized as follows: For Type I, we use the formula (15); for Type II, we use the formula (17) or (22); for Type III, we use the formula (14). We refer the readers to [7, 8] for the details about the computation of the integrals.

4. Error estimates

We analyze our proposed method in this section. For simplicity, we consider the homogeneous Dirichlet boundary condition, i.e., $g = 0$. In fact, we can get the same conclusion as $g \neq 0$. We define the dual volume element space W_h^* of the bilinear finite element space $W_h \subset H_0^1(\Omega)$,

$$W_h^* = \{v \in L^2(\Omega) : v|_{V_{i,j}} = \text{constant}, \ \forall V_{i,j} \in T_h^*\}.$$

Let $I_h : C(\Omega) \to W_h$ and $I_h^* : C(\Omega) \to W_h^*$ be the usual interpolation operators, i.e.,

$$I_h q = \sum_{(x_i, y_j) \in N_h} q_{i,j} \phi_{i,j}(x, y) \text{ and } I_h^* q = \sum_{(x_i, y_j) \in N_h} q_{i,j} \chi_{i,j}(x, y),$$

where

$$\chi_{i,j}(x, y) = \begin{cases} 1 & (x, y) \in V_{i,j}, \\ 0 & \text{elsewhere}, \end{cases}$$

$q_{i,j} = q(x_i, y_j)$, and $\phi_{i,j}(x, y)$ is defined as (12).

Then, (cf. [4, 21])

$$(23) \qquad |q - I_h q|_{H^m(\Omega)} \leq Ch^{2-m} |q|_{H^2(\Omega)} \quad \forall q \in C(\Omega), \quad m = 0, 1.$$

$$(24) \qquad |q_h - I_h^* q_h|_{L^2(\Omega)} \leq Ch |q_h|_{H^1(\Omega)} \quad \forall q_h \in W_h.$$

We multiply both sides of (8) by a test function $v \in H_0^1(\Omega)$ and integrate over Ω to get the weak form. The problem is then to find $q \in H_0^1(\Omega)$ such that

$$(25) \qquad a(q, v) = (\tilde{f}, v) \quad \forall v \in H_0^1(\Omega),$$

where the bilinear form $a(q, v) = \int_\Omega \nabla q \cdot \nabla v dx dy$, $\tilde{f} = f(x, y) + H(\varphi(x, y)) \Delta u_\rho(x, y)$.

The finite element approximation q_h of (25) is defined as a solution to the following problem: Finding $q_h \in W_h$ such that

$$(26) \qquad a(q_h, v_h) = (\tilde{f}, v_h) \quad \forall v_h \in W_h,$$

where the bilinear form $a(q_h, v_h) = \int_\Omega \nabla q_h \cdot \nabla v_h dx dy$.

Multiply (13) by $v_{i,j}$ and add all the terms, we obtain

$$- \sum_{(x_i, y_j) \in N_h} v_{i,j} \int_{\partial V_{i,j}} \nabla q_h \cdot n ds = - \sum_{(x_i, y_j) \in N_h} v_{i,j} \int_{V_{i,j}} \tilde{f} dx dy.$$

Then the bilinear form $a(q_h, I_h^* v_h) = -\sum\limits_{(x_i, y_j) \in N_h} v_{i,j} \int_{\partial V_{i,j}} \nabla q_h \cdot n ds$.

Let us introduce the following discrete norms:

$$|q_h|_{L^2(\Omega),h} = \left(\sum_{(x_i, y_j) \in N_h} \text{meas}(V_{i,j}) q_{h,ij}^2 \right)^{1/2},$$

$$|q_h|_{H^1(\Omega),h} = \left(\sum_{(x_i, y_j) \in N_h} \sum_{(x_m, y_n) \in \Pi(i,j)} \text{meas}(V_{i,j})(q_{h,ij} - q_{h,mn})/d_{ij,mn} \right)^{1/2},$$

$$\|q_h\|_{1,h}^2 = |q_h|_{L^2(\Omega),h}^2 + |q_h|_{H^1(\Omega),h}^2,$$

where $d_{ij,mn}$ is the distance between (x_i, y_j) and (x_m, y_n), and $\Pi(i,j)$ is the index set of those vertices that along with (x_i, y_j), which are in some element of T_h.

Lemma 4.1. *([6, 13]) There exist two positive constants C_0, $C_1 > 0$, independent of h, such that*

$$C_0 |q_h|_{L^2(\Omega),h} \leq \|q_h\|_{L^2(\Omega)} \leq C_1 |q_h|_{L^2(\Omega),h} \quad \forall q_h \in W_h,$$

$$C_0 \|q_h\|_{H^1(\Omega),h} \leq \|q_h\|_{H^1(\Omega)} \leq C_1 \|q_h\|_{H^1(\Omega),h} \quad \forall q_h \in W_h.$$

Lemma 4.2. *([6, 13]) There exist two positive constants C_0, $C_1 > 0$, independent of h and $h_0 > 0$, such that for all $0 < h \leq h_0$,*

$$(27) \qquad |a(q_h, I_h^* v_h)| \leq C_1 \|q_h\|_{H^1(\Omega),h} \|v_h\|_{H^1(\Omega),h} \quad \forall q_h, v_h \in W_h,$$

$$(28) \qquad a(q_h, I_h^* v_h) \geq C_0 \|q_h\|_{H^1(\Omega),h}^2 \quad \forall q_h, v_h \in W_h.$$

This lemma guarantees the existence and uniqueness of the IFVE solution.

Lemma 4.3. *For any q_h, $v_h \in W_h$, we have*

$$(29) \qquad a(q_h, v_h) = a(q_h, I_h^* v_h) + E_h(q_h, v_h).$$

with

$$E_h(q_h, v_h) = \sum_{K \in T_h} \int_{\partial K} (\nabla q_h \cdot n)(v_h - I_h^* v_h) ds.$$

Moreover, there is a positive constant $C > 0$, independent of h, such that

$$(30) \qquad |E_h(q_h, v_h)| \leq Ch \parallel q_h \parallel_{H^1(\Omega),h} \parallel v_h \parallel_{H^1(\Omega),h}.$$

Proof. For each $K \in T_h$ with vertices $\mathbf{x}_k$, $\mathbf{x}_l$, $\mathbf{x}_m$, $\mathbf{x}_n$, we use K_k, K_l, K_m, K_n to denote a quasi-uniform rectangle formed by γ_{kl} and the edges of K, $\mathbf{x}_{kl}$ denotes the midpoint of the edge $\overline{\mathbf{x}_k \mathbf{x}_l}$, see Fig. 5 for the sketch.

Due to $q_h \in W_h$, we find $-\Delta q_h = 0$. It follows by multiplying by $I_h^* v_h$ and integrating on K that:

$$(31) \quad -\int_K \Delta q_h I_h^* v_h dx dy = -\sum_{i=k,l,m,n} \int_{K_i} \Delta q_h I_h^* v_h dx dy$$

$$= -\int_{\partial K} (\nabla q_h \cdot n) I_h^* v_h ds - v_k \int_{\gamma_{nk} + \gamma_{kl}} \nabla q_h \cdot n ds - v_l \int_{\gamma_{kl} + \gamma_{lm}} \nabla q_h \cdot n ds$$

$$- v_m \int_{\gamma_{lm} + \gamma_{mn}} \nabla q_h \cdot n ds - v_n \int_{\gamma_{mn} + \gamma_{nk}} \nabla q_h \cdot n ds.$$
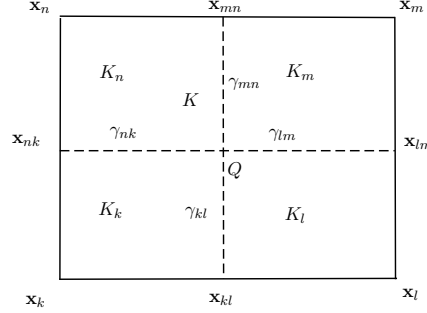
FIGURE 5. The element K.

Similarly,

$$(32) \qquad -\int_K \Delta q_h v_h dxdy = -\int_{\partial K} (\nabla q_h \cdot n) v_h ds + \int_K \nabla q_h \cdot \nabla v_h dxdy.$$

Thus, from (31) and (32), we have:

$$\int_K \nabla q_h \cdot \nabla v_h dxdy = -v_k \int_{\gamma_{nk}+\gamma_{kl}} \nabla q_h \cdot nds - v_l \int_{\gamma_{kl}+\gamma_{lm}} \nabla q_h \cdot nds$$

$$-v_m \int_{\gamma_{lm}+\gamma_{mn}} \nabla q_h \cdot nds - v_n \int_{\gamma_{mn}+\gamma_{nk}} \nabla q_h \cdot nds + \int_{\partial K} (\nabla q_h \cdot n)(v_h - I_h^* v_h) ds.$$

For the proof of (30), c.f. Lemma 3.1 in [5]. □

Theorem 4.1. *Assume that T_h is regular and $q \in H_0^1(\Omega)$ and $q_h \in W_h$ are the solutions of (11) and (13), respectively. If the solution q satisfies $q \in H^2(\Omega)$ and $\tilde{f} \in L^2(\Omega) \cap H^1(\Omega \backslash \Gamma)$, then*

$$(33) \qquad ||q - q_h||_{H^1(\Omega)} \le Ch(||q||_{H^2(\Omega)} + ||\tilde{f}||_{L^2(\Omega)}),$$

$$(34) \qquad ||q - q_h||_{L^2(\Omega)} \le Ch^2(||q||_{H^2(\Omega)} + ||\tilde{f}||_{H^1(\Omega \backslash \Gamma)}).$$

Proof. By (29), (23), (24) and (30), let $\rho_h = I_h q - q_h$,

$$\begin{aligned} ||q - q_h||_{H^1(\Omega)}^2 &= a(q - q_h, q - I_h q) + a(q - q_h, \rho_h) \\ &= a(q - q_h, q - I_h q) + (\tilde{f}, \rho_h - I_h^* \rho_h) - E_h(q_h, \rho_h) \\ &\le Ch||q - q_h||_{H^1(\Omega)}||q||_{H^2(\Omega)} + Ch||\tilde{f}||_{L^2(\Omega)}||\rho_h||_{H^1(\Omega),h} \\ &\quad + Ch||q_h||_{H^1(\Omega),h}||\rho_h||_{H^1(\Omega),h}. \end{aligned}$$

By Lemma 4.2 and the approximation theory we have

$$||q_h||_{H^1(\Omega),h} \le C||\tilde{f}||_{L^2(\Omega)},$$

$$||\rho_h||_{H^1(\Omega),h} \le ||q - q_h||_{H^1(\Omega)} + Ch||q||_{H^2(\Omega)}.$$

The proof of (33) is then completed.

To obtain the L^2 error estimate, we use the standard dual argument. Let $r \in H_0^1(\Omega)$ be the unique function satisfying

$$(35) \qquad -\Delta r = q - q_h \quad \forall (x, y) \in \Omega, \text{ and } r = 0 \text{ on } \partial\Omega.$$

Then we have $\|r\|_{H^2(\Omega)} \le \|q - q_h\|_{L^2(\Omega)}$. By (33) and (29),

$$
\begin{aligned}
\|q - q_h\|^2_{L^2(\Omega)} &= a(q - q_h, r - r_h) + a(q - q_h, r_h) \\
&\le Ch(\|q\|_{H^2(\Omega)} + \|\tilde{f}\|_{L^2(\Omega)})\|r - r_h\|_{H^1(\Omega)} + a(q - q_h, r_h) \\
&\le Ch(\|q\|_{H^2(\Omega)} + \|\tilde{f}\|_{L^2(\Omega)})\|r - r_h\|_{H^1(\Omega)} \\
&\quad + (\tilde{f}, r_h - I_h^* r_h) - E_h(q_h, r_h).
\end{aligned}
$$

As $\mathbf{x}_{kl}$ is the middle point of each edge (see Fig. 5), we have:

$$
\int_K (r_h - I_h^* r_h) ds = 0 \quad \text{for all } K \in T_h.
$$

So that, by (24),

$$
(\tilde{f}, r_h - I_h^* r_h) = \sum_{K \in T_h} (\tilde{f} - \tilde{f}_K, r_h - I_h^* r_h)_K \le Ch^2 \|\tilde{f}\|_{H^1(\Omega\backslash\Gamma)} \|r_h\|_{H^1(\Omega),h}.
$$

Here, if K is an non-interface element, $\tilde{f}_K$ is the average value of $\tilde{f}$ on K; if K is an interface element,

$$
\tilde{f}_K = \begin{cases} \tilde{f}_K^+ & \text{if } (x,y) \in K^+ \subset \Omega^+, \\ \tilde{f}_K^- & \text{if } (x,y) \in K^- \subset \Omega^-, \end{cases}
$$

where $K = K^+ \cup K^-$, and $\tilde{f}_K^+$ and $\tilde{f}_K^-$ are the average values of $\tilde{f}$ on K^+ and K^-, respectively.

And we have

$$
E_h(q_h, I_h r) \le Ch^2 \|q_h\|_{H^1(\Omega),h} \|I_h r\|_{H^1(\Omega),h},
$$

see [21] for the proof.

Thus, by taking $r_h = I_h r$, we get

$$
\begin{aligned}
\|q - q_h\|^2_{L^2(\Omega)} &\le Ch^2(\|q\|_{H^2(\Omega)} + \|\tilde{f}\|_{H^1(\Omega\backslash\Gamma)})\|r\|_{H^2(\Omega)} \\
&\quad + Ch^2 \|\tilde{f}\|_{H^1(\Omega\backslash\Gamma)} \|q - q_h\|_{L^2(\Omega)} \\
&\le Ch^2(\|q\|_{H^2(\Omega)} + \|\tilde{f}\|_{H^1(\Omega\backslash\Gamma)})\|q - q_h\|_{L^2(\Omega)}.
\end{aligned}
$$

The proof of (34) is completed. ∎

5. Numerical experiments

We present two numerical examples in this section to show the convergence results of IFVE method proposed in this paper. We define e_∞, e_0, e_1 as the errors in the L^∞, L^2 norms and semi-H^1 norm, respectively,

$$
e_\infty = \max_{(x_i, y_j) \in \Omega} |u(x_i, y_j) - u_h(x_i, y_j)|,
$$

$$
e_0 = h \left(\sum_{(x_i, y_j) \in \Omega} |u(x_i, y_j) - u_h(x_i, y_j)|^2 \right)^{\frac{1}{2}},
$$

$$
e_1 = h \left(\sum_{(x_i, y_j) \in \Omega} |u_x(x_i, y_j) - u_{h,x}(x_i, y_j)|^2 + |u_y(x_i, y_j) - u_{h,y}(x_i, y_j)|^2 \right)^{\frac{1}{2}},
$$

where $u_{h,x}(x_i, y_j)$ is defined as follows, i.e.,

$$u_{h,x}(x_i, y_j) \approx$$
$$\begin{cases} \dfrac{u_{h,i+1,j} - u_{h,i,j}}{h} & \text{if } \overline{x_i x_{i+1}} \cap \Gamma = \varnothing, \\[2mm] \dfrac{(u_{h,i+1,j} - u_\rho(x_{i+1}, y_j)) - u_{h,i,j}}{h} & \text{if } \overline{x_i x_{i+1}} \cap \Gamma \neq \varnothing \text{ and } u_{h,i+1,j} \in \Omega^+, \\[2mm] \dfrac{u_{h,i+1,j} - (u_{h,i,j} - u_\rho(x_i, y_j))}{h} & \text{if } \overline{x_i x_{i+1}} \cap \Gamma \neq \varnothing \text{ and } u_{h,i+1,j} \in \Omega^-, \end{cases}$$

where $u_{h,i,j} = u_h(x_i, y_j)$.

The derivative $u_{h,y}(x_i, y_j)$ is defined as similar. We define the functions u^+, u^- as follows,

$$u(x,y) = \begin{cases} u^+(x,y) & \text{if } (x,y) \in \Omega^+ \cup \Gamma, \\ u^-(x,y) & \text{if } (x,y) \in \Omega^-. \end{cases}$$

Example 1. *The level set function $\varphi(x,y)$ and the solution $u^\pm$ are given by*

$$\varphi(x,y) = \sqrt{x^2 + y^2} - 0.5, \qquad u^+ = \ln(x^2 + y^2), \qquad u^- = \sin(x + y),$$

see Fig. 6 for a solution plot, the domain, and the interface. The source term $f(x,y)$ and the Dirichlet boundary data $g(x,y)$ are determined from the exact solution $u^\pm(x,y)$.
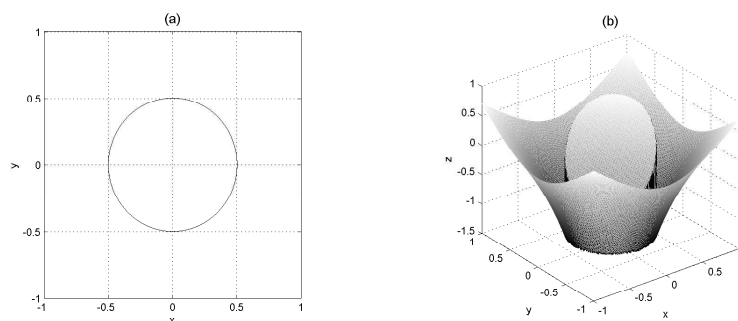
FIGURE 6. (a) The domain and interface of Example 1. (b) A plot of the exact solution of Example 1.

In Table 1, we show a grid refinement analysis. The first column is the mesh size h. The third column is the estimated order of convergency using the formula

$$order = \frac{\log(e_{\infty,N}/e_{\infty,2N})}{\log 2},$$

where N is the number of intervals in x or y directions. The fifth and seventh columns are similar but with L^2 and semi-H^1 norms, respectively. We can see clearly second order convergence in the L^∞, L^2 norms, and first order in the semi-H^1 norm as expected.

Example 2. *The solution $u^\pm$ are the same as Example 1. But the interface which is the zero level set of $\varphi(x,y)$ is complicated, where*

$$\varphi(r,\theta) = r - 0.5 - 0.1\sin(5\theta) \quad \theta \in (0, 2\pi),$$

TABLE 1. A grid refinement analysis of the immersed finite volume element (IFVE) method for Example 1.

h	e_∞	order	e_0	order	e_1	order
1/10	4.066×10^{-3}		3.205×10^{-3}		3.476×10^{-1}	
1/20	1.208×10^{-3}	1.75	9.128×10^{-4}	1.81	1.614×10^{-1}	1.11
1/40	3.471×10^{-4}	1.80	2.431×10^{-4}	1.91	7.885×10^{-2}	1.03
1/80	9.411×10^{-5}	1.88	6.569×10^{-5}	1.89	3.912×10^{-2}	1.01
1/160	2.475×10^{-5}	1.93	1.681×10^{-5}	1.97	1.952×10^{-2}	1.00

where $\tan\theta = x/y$, see Fig. 7 for a plot of the solution, the domain, and the interface.
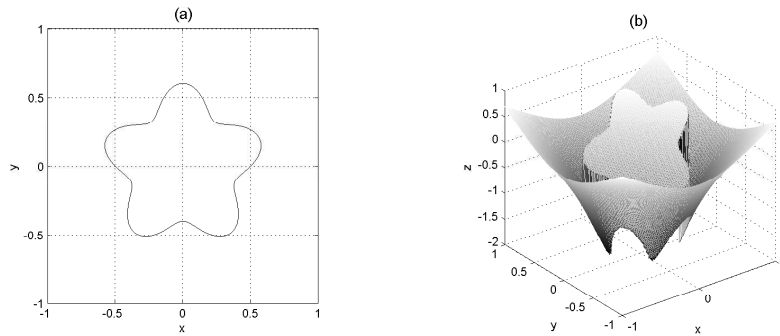
FIGURE 7. (a) The domain and interface of Example 2. (b) A plot of the exact solution of Example 2.

TABLE 2. A grid refinement analysis of the immersed finite volume element (IFVE) method for Example 2.

h	e_∞	order	e_0	order	e_1	order
1/10	2.138×10^{-2}		1.123×10^{-2}		3.620×10^{-1}	
1/20	4.965×10^{-3}	2.11	2.531×10^{-3}	2.15	1.672×10^{-1}	1.11
1/40	1.011×10^{-3}	2.30	6.297×10^{-4}	2.01	8.114×10^{-2}	1.04
1/80	2.423×10^{-4}	2.06	1.077×10^{-4}	2.55	4.051×10^{-2}	1.00
1/160	6.534×10^{-5}	1.89	2.849×10^{-5}	1.92	2.019×10^{-2}	1.00

In Table 2, we can see that although the interface is complicated, IFVE method still has second order convergence in the L^∞, L^2 norms, and first order convergence in the semi-H^1 norm.

At last, we use the linear regression to analyze the data in Table 1, and find that the data obey

$$||u_h - u||_\infty \approx 0.2938h^{1.8403}, \ ||u_h - u||_0 \approx 0.2596h^{1.8946}, \ |u_h - u|_1 \approx 3.6684h^{1.0354}.$$

The data in Table 2 obey

$$||u_h - u||_\infty \approx 2.6348h^{2.1065}, \ ||u_h - u||_0 \approx 1.7402h^{2.1801}, \ |u_h - u|_1 \approx 3.8257h^{1.0374}.$$

See Fig. 8 for these linear regressions. These results further indicate our results.
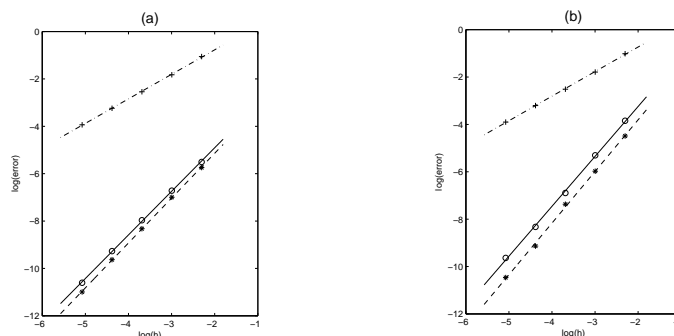
FIGURE 8. (a) The linear regression of the data in Table 1. (b) The linear regression of the data in Table 2. In this diagram, $'\circ'$ denotes L^∞ norm error, the straight line $'-'$ denotes the linear regression for L^∞ norm error, $'*'$ denotes L^2 norm error, the dotted line $'--'$ denotes the linear regression for L^2 norm error, '+' denotes semi-H^1 norm error, the dot dash line $'-.'$ denotes the linear regression for semi-H^1 norm error.

6. Conclusion

In this paper, we have presented IFVE method for Poisson equations with non-homogeneous jump conditions across an arbitrary interface. The method possesses both the advantages of local conservation in the finite volume element method and the capability of IFE method for handling the nonhomogeneous jump conditions across the interface. Particularly, in the interface or the sub-interface dual elements, we do not modify the usual bilinear basis functions, and only modify the right-hand sides of the resulting linear system of equations, which greatly reduces the complexity of the numerical method, and speeds-up the entire algorithm. The resulting IFVE scheme is simple to implement and maintains the data structure as for a regular problem. We have shown that our proposed method is second order accurate in the L^∞ and L^2 norms, and first order in the semi-H^1 norm.

Acknowledgments

References

[1] J. Adams, P. Swarztrauber and R. Sweet, Fishpack: Efficient Fortran subprograms for the solution of separable elliptic partial differential equations, http://www.netlib.org/fishpack/.

[2] J. Bedrossian, J. H. von Brecht, S. Zhu, E. Sifakis and J. M. Teran, A second order virtual node method for elliptic problems with interfaces and irregular domains, J. Comput. Phys., 229 (2010) 6405-6426.

[3] R. Caiden, R. P. Fedkiw and C. Anderson, A numerical method for two-phase flow consisting of separate compressible and incompressible regions, J. Comput. Phys., 166 (2001) 1-27.

[4] P. G. Ciarlet, The finite element methods for elliptic problems, Elsevier, North Holland, 1978.

[5] R. E. Ewing, Z. Li, T. Lin and Y. Lin, The immersed finite volume element methods for the elliptic interface problems, Math. Comput. Simulat., 50 (1999) 63-76.

[6] R. E. Ewing, T. Lin and Y. P. Lin, On the accuracy of the finite volume element method based on piecewise linear polynomials, SIAM J. Numer. Anal., 39 (2002) 1865-1888.

[7] Y. Gong, B. Li and Z. Li, Immersed-interface finite-element methods for elliptic interface problems with nonhomogeneous jump conditions, SIAM J. Numer. Anal., 46 (2008) 472-495.

[8] X. M. He, T. Lin and Y. Lin, A bilinear immersed finite volume element method for the diffusion equation with discontinuous coefficient, Commun. Comput. Phys., 6 (2009) 185-202.

[9] X. M. He, T. Lin and Y. Lin, Immersed finite element methods for elliptic interface problems with non-homogeneous jump conditions, Int. J. Numer. Anal. Model., 8 (2011) 284-301.

[10] S. M. Hou and X. D. Liu, A numerical method for solving variable coefficient elliptic equation with interfaces, J. Comput. Phys., 202 (2005) 411-445.

[11] J. K. Hunter, Z. Li and H. Zhao, Reactive autophobic spreading of drops, J. Comput. Phys., 183 (2002) 335-366.

[12] R. J. LeVeque and Z. Li, The immersed interface method for elliptic equations with discontinuous coefficients and singular sources, SIAM J. Num. Anal., 31 (1994) 1019-1044.

[13] R. H. Li, Z. Y. Chen and W. Wu, Generalized difference methods for differential equations: Numerical analysis of finite volume methods, Marcel Dekker, New York, 2000.

[14] Z. Li, The immersed interface method using a finite element formulation, Appl. Numer. Math., 27 (1998) 253-267.

[15] Z. Li and K. Ito, The immersed interface method, SIAM, 2006.

[16] Z. Li, T. Lin and X. Wu, New cartesian grid methods for interface problems using the finite element formulation, Numer. Math., 96 (2003) 61-98.

[17] Z. Li and S. R. Lubkin, Numerical analysis of interfacial two-dimensional stokes flow with discontinuous viscosity and variable surface tension, Int. J. Numer. Meth. Fluid., 37 (2001) 525-540.

[18] Z. Li, W. C. Wang, I. L. Chern and M. C. Lai, New formulations for interface problems in polar coordinates, SIAM J. Sci. Comput., 25 (2003) 224-245.

[19] T. G. Liu, B. C. Khoo and K. S. Yeo, Ghost fluid method for strong shock impacting on material interface, J. Comput. Phys., 190 (2003) 651-681.

[20] X. D. Liu, R. P. Fedkiw and M. Kang, A boundary condition capturing method for possions equation on irregular domains, J. Comput. Phys., 160 (2000) 151-178.

[21] J. Lv and Y. Li, L^2 error estimate of the finite volume element methods on quadrilateral meshes, Adv. Comput. Math., 33 (2010) 129-148.

[22] C. S. Peskin, The immersed boundary method, Acta Numer., 11 (2002) 479-517.

[23] G. J. Wagner, S. Ghosal and W. K. Liu, Particulate flow simulations using lubrication theory solution enrichment, Int. J. Numer. Meth. Eng., 56 (2003) 1261-1289.

[24] H. Xie, Z. Li and Z. H. Qiao, A finite element method for elasticity interface problems with locally modified triangulations, Int. J. Numer. Anal. Model., 8 (2011) 189-200.

[25] S. Zhao and G.W. Wei, Matched interface and boundary (MIB) for the implementation of boundary conditions in high-order central finite differences, Int. J. Numer. Meth. Eng., 77 (2009) 1690-1730.

[1] Jiangsu Provincial Key Laboratory for Numerical Simulation of Large-Scale Complex Systems, School of Mathematical Science, Nanjing Normal University, Nanjing 210046, China

E-mail: `zhangzhiyue@njnu.edu.cn (Corresponding author)`

[2] Department of Mathematics and Physics, Jiangsu University of Science and Technology, Zhenjiang 212003, China

E-mail: `zhuling327@gmail.com`

[3] Center for Research in Scientific Computation and Department of Mathematics, North Carolina State University, Raleigh, NC 27695-8205, USA

E-mail: `zhilin@math.ncsu.edu`